IEEE Access
Multidisciplinary | Rapid Review | Open Access Journal

SPECIAL SECTION ON ADVANCES IN CHANNEL CODING FOR 5G AND BEYOND

Received November 6, 2018, accepted November 22, 2018, date of publication November 27, 2018,
date of current version December 27, 2018.

Digital Object Identifier 10.1109/ACCESS.2018.2883576

An Improved Network-Coded Multiple Access for Power-Balanced Non-Orthogonal Multiple Access

PINGPING CHEN[1], (Member, IEEE), LONG SHI[2], (Member, IEEE), LITING GUO[1], ZHIFENG CHEN[1], AND LINHUANG WU[1]

[1]Department of Electronic Information, Fuzhou University, Fuzhou 350108, China
[2]Department of Science, Singapore University of Technology and Design, Singapore 487372

Corresponding author: Linhuang Wu (wlh173@163.com)

This work was supported in part by the NSF of China under Grant 61871132, Grant 61671153, and Grant 61401099, in part by the Fujian University Distinguished Researcher Fund 2017, in part by the Fuzhou University Fund under Grant XRC-1601, and in part by the Fujian Educational Technology Project under Grant JAT170087.

ABSTRACT A recently proposed network-coded multiple access (NCMA), consisting of XOR-based channel decoding and multi-user complete decoding (MUD-CD), can significantly improve throughput over conventional successive interference cancellation (SIC) decoding under near power-balanced channels. In this paper, we propose an improved NCMA (I-NCMA) for non-orthogonal multiple access (NOMA) in the 5G wireless communications, consisting of multiple users and a single base station (BS). At the transmitter side, the proposed scheme enables all users to simultaneously transmit messages to the BS in the same time and frequency. At the receiver side, we propose a joint-user channel decoding (JU-CD) to jointly decode all user messages by a single decoder. Then, the extrinsic messages from JU-CD can be jointly utilized by MUD-CD for decoding all user messages. Also, other than conventional NCMA that mainly deals with two users, I-NCMA adapts to the NOMA networks with an arbitrary number of users. Simulation results indicate that the proposed I-NCMA achieves a better decoding performance than both SIC and conventional NCMA over near power-balanced channels in the low-to-medium SNR regime, while retaining a performance close to conventional NCMA in the high SNR regime.

INDEX TERMS NCMA, multi-user complete decoding, NOMA, channel decoding.

I. INTRODUCTION

Compared with the former wireless systems, 5G networks are required to support massive connections with ultra high spectral efficiency. However, these requirements cannot be met by using traditional orthogonal multiple access (OMA) techniques [1]. Driven by this issue, nonorthogonal multiple access (NOMA) is emerging as the key advanced technology in the advanced 5G cellular systems. Accommodating multiple users to the same time and frequency without using orthogonal spreading signatures [1]–[4], NOMA can significantly increase the system throughput compared with existing OMA, e.g., TDMA, FDMA, and OFDMA [5]. For uplink NOMA, multiple users transmit their messages simultaneously to a base station (BS) in the non-orthogonal way. Although the application of NOMA in 5G is relatively new, some enabling solutions of NOMA have been extensively studied in the field of coding and information theory, such as superposition coding [6], successive interference cancellation (SIC), and the message passing algorithm (MPA) [3], [7].

Among various types of receivers in NOMA, SIC has been widely studied because of its simplicity, where serial decision and cancellation were performed [8], [9]. To decode the superposed information at each receiver, the SIC technique was first proposed in [10]. Later on, [11] investigated SIC with OFDM and MIMO, and [12] investigated the decoding process of SIC for the superimposed messages. In SIC-aided NOMA, different users are clustered into different groups, where the users in the same group transmit over the same resource. Notably, successful decoding of SIC relies on a condition that the received powers of different user groups at the BS are significantly different. In particular, [13] unveiled that SIC-aided NOMA should pair a strong user with a weak user as a two-user group to improve the system throughput. In this way, the BS first decodes the strong users message

and then removes this message from its observation before decoding the weak users message.

Note that SIC-aided NOMA with the optimal power allocation has relied on the assumption of perfect channel state information at transmitter (CSIT) which is difficult to obtain in practice [14], [15]. Moreover, the practical communication scenarios hardly guarantees the ideal user grouping required in SIC-aided NOMA, especially when there is a disparity between the numbers of weak users and strong users [16]. Fig. 1 shows an illustrating example where users are uniformly located around a BS. In this case, the number of weak users is larger than that of strong users, since the peripheral area is larger than the area near the BS. Then, the weak users are grouped together and their received powers at the BS are nearly balanced. We refer to this communication scenario as the near power-balanced scenario, where SIC-aided NOMA may not work well. From the information-theoretical perspective, this is positive news in that the users are desirably grouped, even though their received powers at the BS are nearly balanced, since the user grouping can contribute to large rate gain [16]. This rate gain cannot be easily achieved by conventional SIC due to little channel distinctions. To achieve this rate gain, network-coded multiple access (NCMA) proposed in [17]–[20] deployed XOR-based channel decoding (XOR-CD) and multiuser complete decoding (MUD-CD) in the PHY-layer, integrated with the MAC-layer channel coding to introduce correlations among PHY-layer messages.

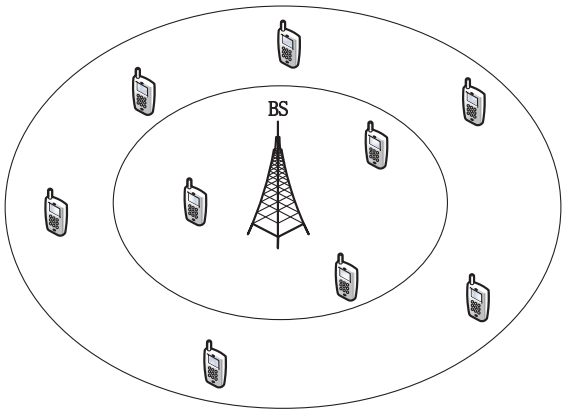

FIGURE 1. An example of NOMA with one BS and multiple uniformly distributed users.

As an efficient decoding technique in the physical-layer network coding (PNC) systems [23]–[26], XOR-CD first maps overlapped channel-coded bits from the users to the XOR bits and then performs channel decoding, while MUD-CD first demodulates the superimposed signals and then performs channel decoding to obtain each individual user message. Moreover, rate-diverse NCMA was proposed to accommodate different modulations for different weak users [16]. Apart from NCMA, recent works have advanced PNC in the multi-user networks [30]–[32], where multiple network-coded (NC) messages are computed from the superimposed packets at the receiver. It is notable that NCMA can also compute multiple NC messages for each overlapped signal under favourable channel conditions.

Superior to SIC, XOR-CD performs better when the received powers from different users are balanced or nearly balanced, while SIC suffers poor performance in this case. As an illustration, ref. [17] showed that in two-user NCMA, XOR-CD can still decode a NC message at SNR of 8.5 dB in a software-defined radio prototype under near power-balanced scenarios, while the MUD-CD/SIC decoder cannot decode the individual user messages with high probability in this case. Fig. 2 plots the PNC rates of XOR-CD and MUD-CD with BPSK over two-user AWGN (power-balanced) channels, respectively. In this figure, the achievable rate of the point-to-point communication with BPSK is also plotted as an upper bound.

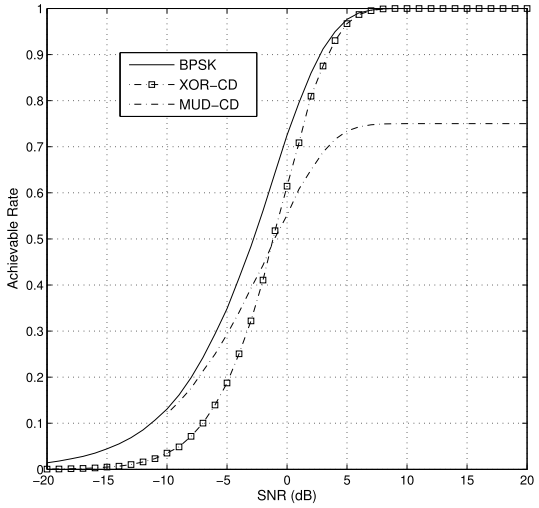

FIGURE 2. PNC rates of XOR-CD, MUD-CD, and upper bound over power-balanced AWGN channels.

First, we observe that XOR-CD outperforms MUD-CD in the high SNR regime, which indicates that MUD-CD suffers a severe rate loss when the power distinction is not significant among users. Second, we observe that there is a considerable rate gap of about 2 dB between the upper bound and XOR-CD in the medium-to-high SNR regime. How to narrow down the gap remains open. Similar to conventional NCMA, we aim to decode each individual user message rather than the NC message [17], [18]. In NCMA, both XOR-CD and MUD-CD are jointly used to recover all user messages.

NCMA can recover any user message that cannot be decoded by MUD-CD, with the aid of the XOR-CD message and the other successfully decoded user message. It is worth noting that the failure of any two decoded messages will result in the loss of at least one user message [16]. To address this issue, this paper proposes an improved NCMA (I-NCMA) that deploys joint-user-channel-decoding (JU-CD) and MUD-CD in NOMA. The main contributions of this work are summarized as follows:

1) The proposed JU-CD is built upon the idea of the joint channel-decoding and network-coding (JCNC). Unlike that the existing JCNC restricts to only two-user transmission [27], [28], the proposed JU-CD can effectively support a general NOMA system with an arbitrary number of users. Particularly, JU-CD can simplify the decoder implementation by decoding all user message with a single decoder, while XOR-CD only decodes NC message of the user messages.
2) Combining JU-CD and MUD-CD, we put forth I-NCMA where the soft information from JU-CD can be utilized by MUD-CD to realize individual user decoding under the near power-balanced scenarios. Simulation results show that I-NCMA outperforms SIC and MUD-CD about 0.4 dB and 0.7 dB at the code rate of 0.4 respectively. In particular, I-NCMA can achieve gains of 0.15 dB and 0.2 dB over conventional NCMA in two-user and three-user NOMA, respectively.
3) For K-user NOMA, the proposed I-NCMA has a much reduced decoding complexity as compared to the conventional NCMA. This is because that I-NCMA only requires a single JU-CD and MUD-CD decoders while the number of possible decoders in NCMA increases exponentially with K [16].

The remainder of this paper is organized as follows: Section II presents the related work and system model. Section III first proposes JU-CD and then I-NCMA. Section IV presents the simulated performance to verify the proposed scheme. Finally, Section V concludes this paper.

II. SYSTEM MODEL

In the following discussions, we use a boldface letter to denote a vector and the corresponding italic letter to denote a symbol within the vector. For example, $\mathbf{x}$ is a vector, and x is a symbol within the vector.

A. ENCODING AT USERS

Fig. 3 shows a NOMA system where K users transmit information to a BS simultaneously. Let a length-L binary vector $\mathbf{u}_k$, $k \in \{1, 2, \ldots, K\}$, be the kth user's source message. Then, $\mathbf{u}_k$ is channel-encoded to generate a length-N binary vector $\mathbf{c}_k$, with $\mathbf{c}_k(i)$ being the ith bit in $\mathbf{c}_k$, $i = 1, 2 \ldots, N$.

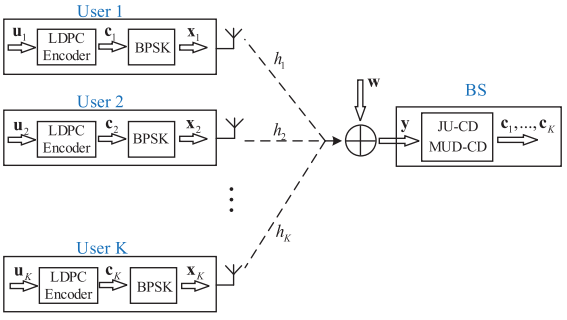

FIGURE 3. System model of uplink NOMA with K users and one BS.

Consider that all users employ the same channel code such that the receiver at BS can decode the desired user messages with the same channel decoder. Finally, the kth user maps $\mathbf{c}_k$ to a signal vector $\mathbf{x}_k$ by the BPSK modulation, with $\mathbf{x}_k(i)$ being the ith element in $\mathbf{x}_k$. We assume that users and BS has the knowledge of parity matrix, and each user transmits with the same power.

Assuming perfect phase synchronization between the users and BS, the received signal at the BS is given by

$$\mathbf{y} = \sum_{k=1}^{K} h_k \mathbf{x}_k + \mathbf{w}, \tag{1}$$

where h_k denotes the channel coefficient between the kth user and BS, and the vector $\mathbf{w}$ contains i.i.d. complex white Gaussian noise samples with zero mean and variance per dimension of $N_0/2$. Note that this paper considers the near power-balanced channels where the received powers from all users at the receiver are nearly balanced. In this scenario, the channel coefficients $h_k, k = 1, 2, \ldots, K$, are almost the same given that the transmit power of each user is the same. Our simulations use the fixed h_k following [33], [34].

With respect to (1), $\tilde{\chi} = \{\sum_{k=1}^{K} h_k x_k | x_k \in \{-1, +1\}\}$ denotes the set of the superimposed signals from K users. Let $\tilde{\mathbf{x}}$ denote the superimposed signal vector from K users (i.e., $\mathbf{y}$ with the noise removed), $\tilde{\mathbf{x}}(i) \in \tilde{\chi}$, $i = 1, 2, \ldots, N$. Considering the block fading channels, channel coefficients keep unchanged during one block transmission and vary from one block to next. In general, the cardinality of $\tilde{\chi}$ is 2^K, denoted by $|\tilde{\chi}| = 2^K$ (by cardinality, we mean the number of distinct elements in the set). We then use $\mathbf{c}_{1\sim K}(i) = [\mathbf{c}_1(i), \mathbf{c}_2(i), \ldots, \mathbf{c}_K(i)]$ to denote a joint bit vector, with the ith element $\mathbf{c}_{1\sim K}(i)$ being a binary vector consisting of the coded bits from K users. The set of all joint bits is given by

$$\mathcal{S} = \{[c_1, c_2, \ldots, c_K] | c_k \in \{0, 1\}, k = 1, 2, .., K\}, \tag{2}$$

where $|\mathcal{S}| = 2^K$. As such, $\mathbf{c}_{1\sim K}(i) \in \mathcal{S}$. Note that in general, each element in $\tilde{\chi}$ corresponds to a unique element in $\mathcal{S}$ under the random fading channels. Then, we define the one-to-one mapping between $\mathcal{S}$ and $\tilde{\chi}$ as ξ: $\mathcal{S} \rightarrow \tilde{\chi}$, i.e., $\tilde{\mathbf{x}}(i) = \xi(\mathbf{c}_{1\sim K}(i))$.

B. DECODING AT BS

In this part, we briefly review the decoding techniques that are widely used in NOMA.

1) SIC-AIDED NOMA

First, the key of SIC is to successively decode the strong users with the larger received SNRs by treating the remaining user groups as noise. In some communications, ensuring large power differences among all user groups is not possible. For example, Fig. 1 shows a practical scenario where the users are uniformly located around the BS, and the area close to the BS is smaller than the peripheral area. Then, the weak users are grouped together, resulting in a larger inter-user interference

to the strong users. In this case, SIC does not perform well due to the accumulated interference from weak group.

Suppose that the received powers from the group of users at BS are almost the same. We refer to this as the near power-balanced scenario. Generally, SIC computes the initial channel message for decoding the packet of stronger user by treating packets of the remaining users as noise. In this case, the effective signal-to-interference-plus-noise ratio (SINR) of user 1 is relatively small due to strong interference from other users. As a result, the SIC decoder cannot retrieve any of the packets. To deal with this near power-balanced scenario, NOMA is in urgent need of a reliable decoding technique.

2) NCMA

PNC was originally proposed to double the throughput of a two-way relay network compared with the conventional store-and-forward relaying [23], [34]. Prior works on channel-coded PNC mainly focused on the relay networks, such as XOR-CD [9], MUD-CD [21], and JCNC [9], [21] operated PNC systems. Recently, NCMA offers a code-domain solution of NOMA, which generalizes the spirit of PNC to the wireless multiple access networks. In particular, Fig. 4 shows the parallel decoding operations of XOR-CD and MUD-CD in conventional NCMA [17].

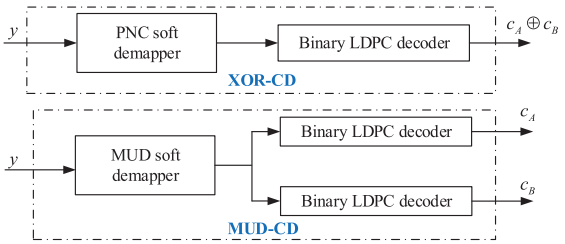

FIGURE 4. Block diagrams of conventional NCMA including XOR-CD and MUD-CD.

NCMA includes decoding operations in both MAC and PHY layers. For each user, the whole message sequence is divided and encoded into multiple packets by an erasure channel code at the MAC layer, which are then channel-encoded in the PHY layer for reliable transmission. At the receiver side, the BS deploys XOR-CD and MUD-CD to decode the received packets in the PHY layer at different time slots. The decoded packets are then collected and passed to the MAC layer for recovery with the help of the erasure code.

In the paper, we focus on decoding operation of NCMA in the PHY layer, as the joint use of XOR-CD and MUD-CD in this layer plays a vital role in NCMA. First, we propose JU-CD to jointly decode all user messages within a single decoder at the BS. Then, we propose I-NCMA by jointly exploiting JU-CD and MUD-CD. Compared with NCMA, I-NCMA employs JU-CD rather than XOR-CD to help MUD-CD to decode the messages of each user.

For ease of understanding, we present a simple example to illustrate the decoding process in NCMA. Consider a two-user NCMA scheme where two user transmit $\mathbf{x}_1$ and $\mathbf{x}_2$ to

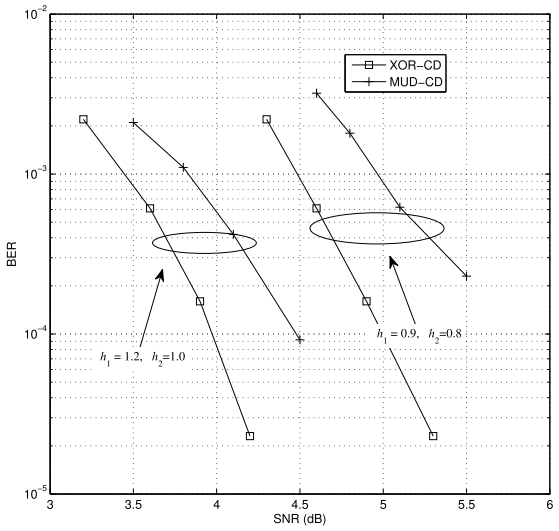

FIGURE 5. BER performance of XOR-CD and MUD-CD in two-user NOMA with $(h_1, h_2) = (1.2, 1.0)$ and $(h_1, h_2) = (0.9, 0.8)$.

the BS simultaneously. On one hand, MUD-CD in NCMA attempts to decode both channel-coded $\mathbf{c}_1$ and $\mathbf{c}_2$ upon receiving $\mathbf{y}$ in (1). On the other hand, XOR-CD attempts to decode $\mathbf{c}_\tau = \mathbf{c}_1 \oplus \mathbf{c}_2$ (the bit-wise XOR of $\mathbf{c}_1$ and $\mathbf{c}_2$) based on the same overlapped signals. To be specific, XOR-CD first maps the overlapped signals into the XOR of the channel-coded bits. Channel decoding is then applied to obtain the XOR of the user messages. By MUD-CD and XOR-CD, we can obtain three decoded codewords $\mathbf{c}_1, \mathbf{c}_2$ and $\mathbf{c}_\tau$. The key decoding principle of NCMA is that any single codeword can be recovered by the other two codewords if the two codewords are successfully decoded, i.e, $\mathbf{c}_i = \mathbf{c}_j \oplus \mathbf{c}_k$, $i \neq j \neq k, i, j, k \in \{1, 2, \tau\}$.

Now it is clear that the decoding of NCMA will fail if any two codewords are not successfully decoded. In fact, in the near power-balanced communications, it is difficult for MUD-CD to achieve successful decoding of both $\mathbf{c}_1$ and $\mathbf{c}_2$ when received powers of two users are almost the same. However, we can obtain the XOR message to contribute to decoding both user messages in NCMA. To illustrate this problem, Fig. 5 compares the decoding performance of XOR message in XOR-CD and MUD-CD, where two users adopt the same (273, 191) finite geometry (FG)-LDPC code [35] in the near power-balanced scenarios where $(h_1, h_2) = (1.2, 1.0)$ and $(h_1, h_2) = (0.9, 0.8)$, respectively. In this figure, we observe that XOR-CD yields a significant gain over MUD-CD. This result coincides with the PNC rates in Fig. 2, which indicates that XOR-CD has a larger achievable rate than MUD-CD in the high SNR regime.

III. PROPOSED I-NCMA SYSTEM

As we illustrated, XOR-CD in NCMA only decodes the XOR of user messages rather than each individual user message. First, we propose JU-CD to jointly decode all users messages by a single decoder. Different from XOR-CD that computes

the soft information of XOR messages, JU-CD computes and iteratively updates soft information of all combinations of all user messages. Indeed, JU-CD builds on top of JCNC, originally proposed as the channel-coded PNC technique in two-way relay networks [27], [28]. Going beyond, the proposed JU-CD caters to the general NOMA network with an arbitrary number of users. Second, we show that the proposed JU-CD can enhance the decoding performance of NCMA.

A. PROPOSED JU-CD

Recall that $\mathbf{c}_{1\sim K}$ is a joint bit vector of K users and its ith element $\mathbf{c}_{1\sim K}(i)$ is a bit vector of the K users, $i = 1, 2, \ldots, N$. Thus, $\mathbf{c}_{1\sim K}(i)$ has 2^K different combinations, $\mathbf{c}_{1\sim K}(i) \in \mathcal{S}$. Since all users adopt the same channel code, $\mathbf{c}_{1\sim K}(i)$ can be decoded by the same channel decoder that for each individual user. We define the soft message of $\mathbf{c}_{1\sim K}(i)$ passing within iterative decoder as a length-2^K probability vector $\mathbf{p}^i$.

For simplicity, we use η to denote the conversion from a binary vector to its corresponding decimal value $o = \eta(\mathbf{c}_{1\sim K}(i)) = \eta([\mathbf{c}_1(i), \mathbf{c}_2(i), \ldots, \mathbf{c}_K(i)])$. Then, $o \in \Delta = \{0, 1, \ldots, 2^K - 1\}$. Conversely, we use $\eta_k^{-1}(o)$ to denote the kth bit in the bit vector converted from o, $k = 1, 2, \ldots, K$.[1] Accordingly, $p^i(o)$ denotes the probability of $\mathbf{c}_{1\sim K}(i) = \eta^{-1}(o)$. Recall that each $\mathbf{c}_{1\sim K}(i)$ is associated with a received superimposed point $\tilde{\mathbf{x}}(i) \in \tilde{\chi}$, i.e., $\tilde{\mathbf{x}}(i) = \xi(\mathbf{c}_{1\sim K}(i))$.

The iterative decoder is performed within a parity matrix that consists of two sets of nodes, variable nodes $\mathbf{v}$ and check nodes $\mathbf{t}$. A variable node $\mathbf{v}(i)$ corresponds to a joint bit vector $\mathbf{c}_{1\sim K}(i)$. We note that parity matrix for decoding the joint bit vector $\mathbf{c}_{1\sim K}$ is the same as that for decoding each user message. The proposed JU-CD adopts sum product algorithm (SPA). Then the initial message of each variable node from the received signal $\mathbf{y}$ in (1) is given by

$$\begin{aligned} p^i(o) &= \Pr(\mathbf{y}(i)|\mathbf{c}_{1\sim K}(i), h_1, h_2, \ldots, h_K) \\ &= \Pr(\mathbf{y}(i)|\tilde{\mathbf{x}}(i) = \xi(\mathbf{c}_{1\sim K}(i)), h_1, h_2, \ldots, h_K) \\ &= \Pr(\mathbf{y}(i)|\sum_{k=1}^{K} h_k \mathbf{x}_k(i), h_1, h_2, \ldots, h_K) \\ &= \frac{1}{\beta\pi\sigma^2} \exp\left(- \frac{|\mathbf{y}(i) - \sum_{k=1}^{K} h_k \mathbf{x}_k(i)|^2}{2\sigma^2} \right), \end{aligned} \tag{3}$$

where $i = 1, 2 \ldots, N$ and β is a normalization factor that ensures $\sum_{o=0}^{2^K-1} p^i(o) = 1$. Within the SPA, we define functions VAR and CHK to formulate message updating rules at the variable and check nodes, respectively. We first illustrate the message update of the node with degree three. The messages from the variable nodes with degree greater than three can be recursively calculated by using

$$\begin{aligned} \mathbf{v}^i &= \mathrm{VAR}(\mathbf{p}^1, \ldots, \mathbf{p}^j, \ldots, \mathbf{p}^g) \\ &= \mathrm{VAR}(\mathbf{p}^g, \mathrm{VAR}(\mathbf{p}^1, \ldots, \mathbf{p}^j, \ldots, \mathbf{p}^{g-1})), \end{aligned} \tag{4}$$

[1]For example, if $\mathbf{c}_{1\sim K}(i) = [1\ 1\ 0\ 1]$, then $o = \eta([1\ 1\ 0\ 1]) = 13$. Conversely, $\eta_3^{-1}(13) = 0$.

where $\mathbf{v}$ is a degree-g variable node, $\mathbf{v}^i$ denotes the messages from $\mathbf{v}$ to its ith connected check node, and $\mathbf{p}^j$ denotes the input messages of $\mathbf{v}$, $j = 1, 2, \ldots, g$.

Similarly, the messages from the check nodes with degree of greater than three can be recursively calculated by

$$\begin{aligned} \mathbf{t}^i &= \mathrm{CHK}(\mathbf{q}^1, \ldots, \mathbf{q}^j, \ldots, \mathbf{q}^{d-1}) \\ &= \mathrm{CHK}(\mathbf{q}^{d-1}, \mathrm{CHK}(\mathbf{q}^1, \ldots, \mathbf{q}^j, \ldots, \mathbf{q}^{d-2})), \end{aligned} \tag{5}$$

where $\mathbf{t}$ is a degree-d check node, $\mathbf{t}^i$ denotes the message from $\mathbf{t}$ to its connected the ith variable node, and $\mathbf{q}^j$ denotes the input messages of $\mathbf{t}$, $j = 1, 2, \ldots, d$.

1) OUTPUT MESSAGE OF VARIABLE NODES

Assume that the variable node $\mathbf{v}$ is connected to two check nodes. Given the two input messages $\mathbf{p} = [p(0), p(1), \ldots, p(2^K - 1)]$ from the channel and $\mathbf{p}^1 = [p^1(0), p^1(1), \ldots, p^1(2^K - 1)]$ from the first check node, the outgoing probability message to the second check node, denoted by $\mathbf{v}^2 = [v^2(0), v^2(1), \ldots, v^2(2^K - 1)]$, where $v^2(o)$ denotes the probability of $\mathbf{v} = o$, is given by

$$\begin{aligned} v^2(o) = \Pr(\mathbf{v} = o|p, p^1) &= \frac{\Pr\{p, p^1|\mathbf{v} = o\}\Pr\{\mathbf{v} = o\}}{\Pr\{p, p^1\}} \\ &= \frac{\Pr\{\mathbf{v} = o|p\}\Pr\{\mathbf{v} = o|p^1\}\Pr\{p\}\Pr\{p^1\}}{\mathbf{v}\{\mathbf{v} = o\}\Pr\{p, p^1\}} \\ &= \beta p(o) p^1(o). \end{aligned} \tag{6}$$

In (6), β is a normalization factor that ensures $\sum_{o=0}^{2^K-1} v^2(o) = 1$. Then, the output message $\mathbf{v}^2$ is

$$\mathbf{v}^2 = \mathrm{VAR}(\mathbf{p}, \mathbf{p}^1). \tag{7}$$

2) OUTPUT MESSAGE OF CHECK NODES

Suppose that a check node $\mathbf{t}$ is connected to three variable nodes. We use $\mathbf{q}^1 = [q^1(0), q^1(1), \ldots, q^1(2^K - 1)]$ and $\mathbf{q}^2 = [q^2(0), q^2(1), \ldots, q^2(2^K - 1)]$ to denote the incoming messages from the variable nodes $\mathbf{v}(1)$ and $\mathbf{v}(2)$, respectively. Let $\mathbf{q}' = [q'(0), q'(1), \ldots, q'(2^K - 1)]$ denote the probability of the coded bit $\mathbf{v}'$ from $\mathbf{v}(1)$ and $\mathbf{v}(2)$, where $q'(o)$ denotes the probability of $\mathbf{v}' = o$. We calculate message $\mathbf{q}'$ based on $\mathbf{q}^1$ and $\mathbf{q}^2$, with $q'(o)$ being

$$q'(o) = \Pr(\mathrm{v}' = d|\mathbf{q}^1, \mathbf{q}^2) = \sum_{\substack{\varphi(m,n)=o, \\ m,n\in\Delta}} q^1(m) q^2(n), \tag{8}$$

where $\varphi(m, n) = o$, the bit-wise parity-check function of JU-CD, will be defined in (10), according to the LDPC encoding as blow.

For channel decoding of the kth user, the check node $\mathbf{t}$ is connected to three variable nodes $\mathbf{v}_k(1)$, $\mathbf{v}_k(2)$, and $\mathbf{v}_k(3)$, with their corresponding coded bits satisfying

$$\mathbf{c}_k(1) \oplus \mathbf{c}_k(2) \oplus \mathbf{c}_k(3) = 0, \tag{9}$$

where $k = 1, 2, \ldots, K$. Thus, the encoding of the joint bits in JU-CD also satisfies the same requirement. Suppose that three joint bit vectors corresponding to three

variable nodes are $\mathbf{c}_{1\sim K}(i)(1) = [\mathbf{c}_1(1), \mathbf{c}_2(1), \ldots, \mathbf{c}_K(1)]$, $\mathbf{c}_{1\sim K}(i)(2) = [\mathbf{c}_1(2), \mathbf{c}_2(2), \ldots, \mathbf{c}_K(2)]$, and $\mathbf{c}_{1\sim K}(i)(3) = [\mathbf{c}_1(3), \mathbf{c}_2(3), \ldots, \mathbf{c}_K(3)]$, respectively. Moreover, m, n and o are used to represent the decimal values of the three vectors, i.e., $m = \eta(\mathbf{c}_{1\sim K}(i)(1))$, $n = \eta(\mathbf{c}_{1\sim K}(i)(2))$, and $o = \eta(\mathbf{c}_{1\sim K}(i)(3))$. Thus, with respect to (9), given a value of o, we define $\varphi(m, n) = o$ in (8) as

$$\eta_k^{-1}(m) \oplus \eta_k^{-1}(n) = \eta_k^{-1}(o), \quad k = 1, 2, \ldots, K. \tag{10}$$

As defined before, $\eta_k^{-1}(m)$ is the kth bit of the bit vector converted from a decimal value m. Finally, the output message of $\mathbf{t}$ is

$$\mathbf{t}^3 = \mathrm{CHK}(\mathbf{q}^1, \mathbf{q}^2). \tag{11}$$

3) JOINT USER MAPPING

After iterations, $\mathbf{v}(i)$ is determined as $j \in \Delta$. The *a-posteriori* probability vector of $\mathbf{v}(i)$, denoted by $\boldsymbol{\epsilon} = [\boldsymbol{\epsilon}(0), \boldsymbol{\epsilon}(1), \ldots, \boldsymbol{\epsilon}(2^K - 1)]$, is evaluated in (5) by computing all incoming messages from the check nodes as well as the channel message in (3). Then the joint user mapping is performed by

$$\mathbf{v}(i) = \mathbf{c}_{1\sim K}, \quad \text{if } \underset{\forall i \in \Delta}{\operatorname{argmax}}\, \boldsymbol{\epsilon}(i) = j, \tag{12}$$

where $\mathbf{c}_{1\sim K} = \eta^{-1}(j)$. Finally, we estimate all the user messages, since $\mathbf{c}_{1\sim K} = [\mathbf{c}_1(i), \mathbf{c}_2(i), \ldots, \mathbf{c}_K(i)]$.

B. PROPOSED I-NCMA

Recall that the conventional NCMA exploits the decoded messages based on their hard decoded information. In the proposed I-NCMA, the soft information between JU-CD and MUD-CD are utilized and iterative updated to improve the decoding performance.

In I-NCMA, the *a-posteriori* probability vector of $\mathbf{v}(i)$ from JU-CD is $\boldsymbol{\epsilon} = [\boldsymbol{\epsilon}(0), \boldsymbol{\epsilon}(1), \ldots, \boldsymbol{\epsilon}2^K - 1)]$, where $\boldsymbol{\epsilon}(j)$ denotes the probability of $\mathbf{v}(i) = j$, i.e., $\mathbf{c}_{1\sim K} = \eta^{-1}(j)$ where $\mathbf{c}_k(i) = \eta_k^{-1}(j)$, $j \in \Delta$. Given $\boldsymbol{\epsilon}$, we can further compute the *a-posteriori* information for each user. Let $\bar{\mathbf{L}}_k$ denote the *a-posteriori* log-likelihood ratio (LLR) vector for the kth user. The LLR of the ith element in $\bar{\mathbf{L}}_k$ is given by

$$\bar{\mathbf{L}}_k(i) = \log \frac{\sum\limits_{\eta_k^{-1}(j)=0, j\in\Delta} \epsilon(j)}{\sum\limits_{\eta_k^{-1}(j)=1, j\in\Delta} \epsilon(j)}. \tag{13}$$

where $i = 1, 2, \ldots, N$. We note that soft information of each variable node in the kth user's decoder is one-dimensional while soft information of joint bits updated in JU-CD is multi-dimensional, since JU-CD attempts to decode all user messages within a single decoder.

In the MUD-CD for NOMA, the initial soft information is computed from the channel messages for MUD-CD decoder. In the proposed scheme, the soft information $\bar{\mathbf{L}}_k$ from JU-CD is more reliable than that directly computed from the channel messages. With the initial soft information, MUD-CD performs separate channel decoder to obtain the individual user message. Due to the more reliable initial information, the decoding performance of MUD-CD with the aid of JU-CD is greatly improved as compared to that without JU-CD.

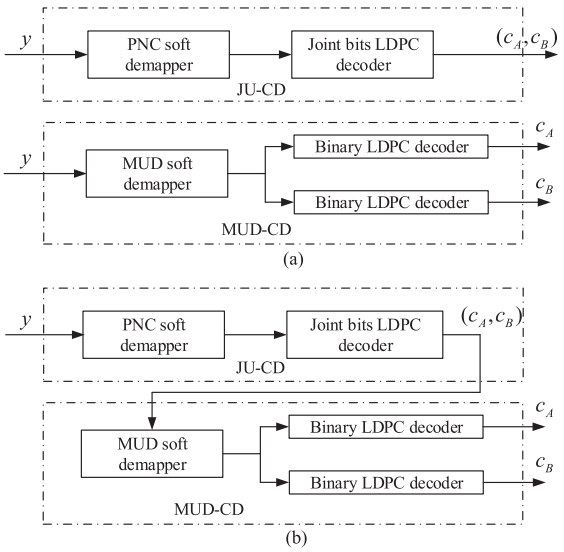

FIGURE 6. Block diagrams of two I-NCMA schemes: (a) IP-NCMA (b) IS-NCMA.

In the following, we construct two types of I-NCMA, i.e., Parallel I-NCMA (IP-NCMA) and Serial I-NCMA (IS-NCMA). As depicted in Figs. 6(a) and (b), IP-NCMA performs JU-CD and MUD-CD in parallel, while IS-NCMA performs JU-CD and MUD-CD in serial. The serial decoding scheme is known to perform better than the parallel one but suffers from more decoding delay [33]. Let $\tilde{\mathbf{L}}_k$ denote the final LLR vector to estimate the kth user's codeword $\mathbf{c}_k$.

1) IP-NCMA

Given the received signal $\mathbf{y}$, we perform MUD-CD and JU-CD in parallel to obtain the *a-posteriori* LLR messages for each user. Assume that *a-posteriori* LLR vector of the kth user from MUD-CD is $\hat{\mathbf{L}}_k$, with $\hat{\mathbf{L}}_k(i)$ being the LLR of the ith coded bits, $i = 1, 2, \ldots, N$. In this scheme, we can simply sum up the LLRs $\hat{\mathbf{L}}_k$ from MUD-CD and $\bar{\mathbf{L}}_k(i)$ from JU-CD to obtain $\tilde{\mathbf{L}}_k$ for the kth user. Thus, the total LLR is given by

$$\tilde{\mathbf{L}}_k(i) = \bar{\mathbf{L}}_k(i) + \hat{\mathbf{L}}_k(i). \tag{14}$$

From (14), the final decision is given by

$$\mathbf{c}_k(i) = \begin{cases} 0, & \text{if } \tilde{\mathbf{L}}_k(i) > 0, \\ 1, & \text{otherwise.} \end{cases} \tag{15}$$

2) IS-NCMA

In this scheme, JU-CD and MUD-CD are operated successively. First, the *a-posteriori* LLR $\bar{\mathbf{L}}_k$ from JU-CD is fed into the MUD-CD, as the initial LLR messages for the kth channel decoder in MUD-CD. Second, the MUD-CD outputs the *a-posteriori* LLR to estimate $\mathbf{c}_k$, which largely follows (15).

C. BEP COMPARISON BETWEEN NCMA AND I-NCMA

This section illustrates the probability of bit error (BEP) comparison between K-user NCMA and I-NCMA. Recall that NCMA consists of XOR-CD and MUD-CD. However, XOR-CD only decodes the XOR of the user messages. Thus, XOR-CD cannot decode any user message if MUD-CD fails to recover all user messages even though the XOR message is successfully decoded. Let P_k denote the BEP of decoding the kth user message by MUD-CD, $k = 1, 2, \ldots, K$, and P_{K+1} denote the BEP of XOR-CD. In total, NCMA has $K+1$ BEPs. According to the decoding principle of NCMA, any K decoding out of $K+1$ successful decodings lead to a full recovery of all K-user messages. Let Ω denote a set that collects all combinations of any distinct K out the $K+1$ BEPs. Thus, the BEP of K-user NCMA is given by

$$\bar{P} = 1 - \sum_{\mathcal{C}\in\Omega} \prod_{i\in\mathcal{C}} (1 - P_i). \tag{16}$$

Next, we analyze the BEP for I-NCMA that consists of JU-CD and MUD-CD. Let P_N denote the BEP of JU-CD. Given that MUD-CD can also decode the kth user's message with BEP of P_k, the complete decoding of all user messages fails if and only if both JU-CD and MUD-CD fail. Then, the BEP of K-user I-NCMA is given by

$$\hat{P} = P_N \prod_{i=1}^{K} P_i. \tag{17}$$

The authors in [28] has shown that JCNC outperforms XOR-CD in all SNR regimes over the two-way relay networks. Moreover, JU-CD is derived from JCNC. The main difference between JU-CD and JCNC lies in that JCNC aims for the XOR of the users messages based on *a-posteriori* probability, while JU-CD aims for the individual user message. Consider a two-user case with $h_1 = 1.2$ and $h_2 = 1.0$, Fig. 7 shows that JCNC achieves gains of 0.3 dB and 0.2 dB over XOR-CD in terms of BER, where two users employ the regular LDPC code with the same rate of 0.25 and 0.4, respectively. Thus, with reference to (16) and (17), it is shown that I-NCMA outperforms NCMA.

IV. SIMULATION RESULTS

In this section, we present simulation results of various LDPC-coded NOMA systems, including SIC/MUD-CD aided NOMA, conventional NCMA and I-NCMA. Each user deploys the AR3A codes in [36], [37]. In our simulation, the information length of each user is set to 1000 bits. The number of decoding iterations is set to 30. Note that we compare the BER performance of the worst user channel in NOMA.

A. BER OF TWO-USER NOMA

Fig. 8 depicts the BER performance for various two-user NOMA systems with code rate 1/2. Recall that, SIC-aided NOMA first decodes the stronger user and then decodes the weaker user after removing the decoded messages of the strong user, while NCMA decodes the bitwise XOR of two user codewords. Consider that $h_1 = 1.1$ and $h_2 = 0.9$. First, we observe that IS-NCMA outperforms NCMA and SIC-aided NOMA. In particular, the gain of IS-NCMA over SIC-based NOMA can be up to 0.4 dB in the low SNR regime, since SIC-aided NOMA may not be able to achieve the potential rate gain of weaker user in the low SNR regime. However, the gain is reduced to 0.2 dB below the BER of 10^{-5}. This gain is useful because various communication systems, such as voice, video (live streaming), interactive gaming, require target BER of round 10^{-5}. Second, we observe that SIC-aided NOMA performs almost the same as NCMA in the high SNR regime, although NCMA offers a gain of 0.2 dB over SIC-aided NOMA in the low SNR regime. This is because that SIC is hard to decode both messages one by one due to

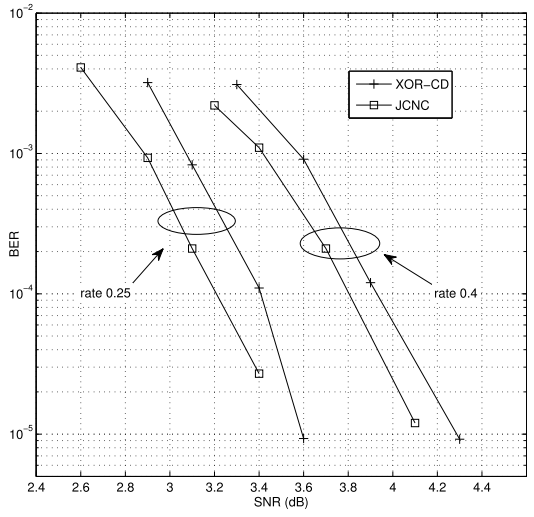

FIGURE 7. BER performance of XOR-CD and JCNC, with $h_1 = 1.2$ and $h_2 = 1.0$.

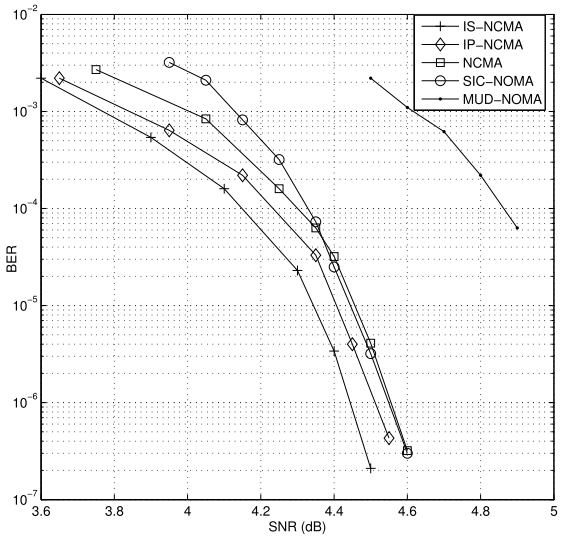

FIGURE 8. BER performance of two-user IS-NCMA, IP-NCMA, NCMA, SIC-NOMA and MUD-CD.

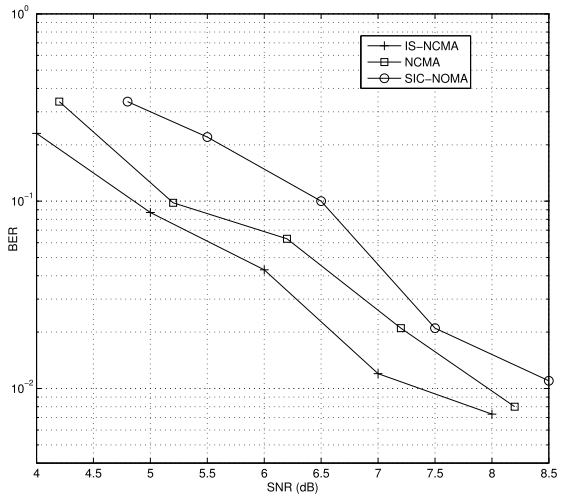

FIGURE 9. BER performance of two-user IS-NCMA, NCMA, and SIC-NOMA over power-balanced channel.

the large noise in low SNR regime. In particular, IS-NCMA still maintains the performance gain of 0.15 dB over SIC-aided NOMA and NCMA when BER is smaller than 10^{-5}. Moreover, MUD-CD performs worst among all schemes in the near power-balanced scenarios.

B. BER OF THREE-USER NOMA

Fig. 10 compares the BER performance among NCMA, SIC-aided NOMA, and IS-NCMA in three-user NOMA. Consider $(h_1, h_2, h_3) = (1.5, 1.4, 1.4)$ and $(1.3, 1.2, 1.1)$, and code rate of 0.4. As for NCMA, XOR-CD decodes the XOR bits of three user messages and MUD-CD decodes three individual user messages. Thus, any single message can be recovered by the other three messages. In IS-NCMA, the *a-posteriori* probability from JU-CD is fed into MUD-CD to decode three user messages. We observe that IS-NCMA outperforms NCMA and SIC-aided NOMA by 0.15 dB and 0.2 dB in the low-to-medium SNR regime, respectively. However, the BER of SIC-aided NOMA approaches that of IS-NCMA for both cases in the high SNR regime. In particular, at $(h_1, h_2, h_3) = (1.3, 1.2, 1.1)$, SIC-aided NOMA performs almost the same as IS-NCMA at BER $= 10^{-4}$ when SNR $= 6.7$ dB. This is because that in decoding one user messages, the other two-user interference is relatively large. As such, SIC first removes the decoded signal of two stronger users before decoding the weakest user, resulting in a slight performance gain over MUD-CD involved I-NCMA. To address this issue, one possible solution is to replace MUD-CD with SIC to combine with JU-CD in I-NCMA, which deserves an intensive study in future.

C. BER OF TWO-USER NOMA WITH QPSK

Fig. 11 compares the BER performance among IS-NCMA, conventional NCMA, SIC-aided NOMA where the binary LDPC code with QPSK modulation are used. The source bits over in-phase and quadrature components of the QPSK symbol are channel-encoded separately using an identical LDPC encoder. In this context, the NC codeword mapped from two user codewords is still a valid LDPC codeword. Correspondingly, the in-phase and quadrature parts of a QPSK packet can be equivalently treated as two independent BPSK packets. Consider $(h_1, h_2) = (1.2, 1.0)$ and code rate of 0.4. We can observe that IS-NCMA achieves gains of 0.2 dB and 0.4 dB over NCMA and SIC-aided NOMA in the low-to-medium SNR regime with 30 iterations, respectively, while the gain of IS-NCMA over SIC-aided NOMA is increased to about 0.5 dB with 5 iterations only. This is due to the fact that IS-NCMA also benefits from faster convergence speed of successful decoding than SIC-aided NOMA.

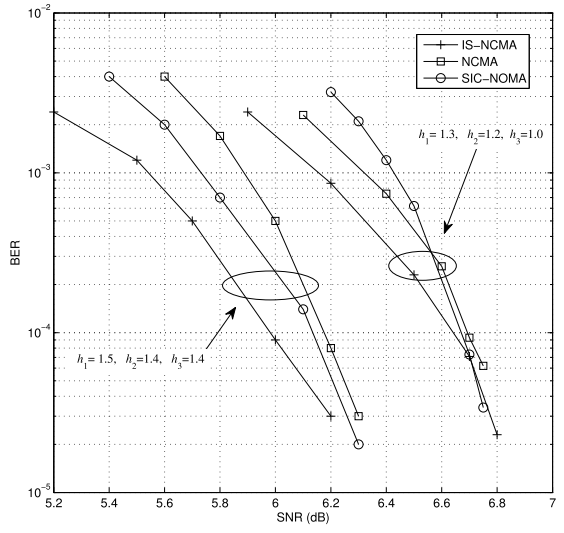

FIGURE 10. BER performance of three-user IS-NCMA, NCMA, and SIC-NOMA.

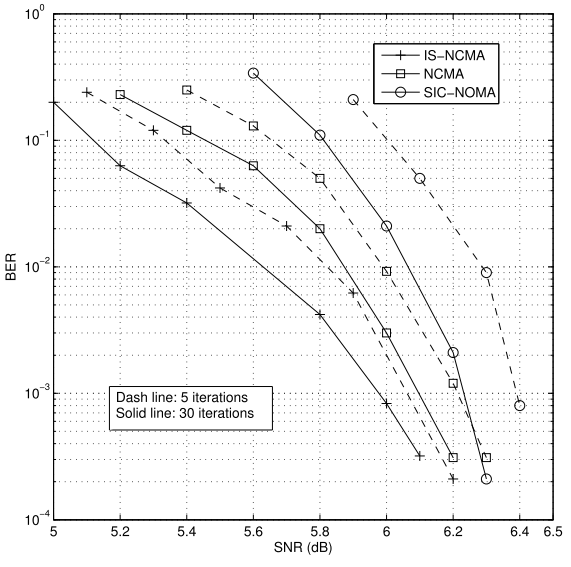

FIGURE 11. BER performance of two-user IS-NCMA, NCMA, and SIC-NOMA with QPSK modulation.

V. CONCLUSIONS

We have proposed a JU-CD decoding that can decode multiple user messages within a single decoder. Based on JU-CD, we constructed an improved NCMA as an alternative solution for power-balanced and near power-balanced NOMA. The key idea of I-NCMA is to jointly exploits JU-CD and MUD-CD to decode concurrent transmissions by multiple users. Thus, we can obtain decoding diversity from the two different decoders. Our simulation results show for near power-balanced scenarios, especially in the low-to-medium SNR regime, I-NCMA is superior to conventional NCMA and SIC-aided NOMA in terms of BER performance. Several interesting directions may follow this paper. First, it is of interest to enhance I-NCMA by taking SIC into consideration when the received powers are diverse. Second, it is desired to design rate-diverse NCMA for power-imbalanced NOMA where the users with different received powers use different code rates.

REFERENCES

[1] L. Dai, B. Wang, Y. Yuan, S. Han, C.-L. I, and Z. Wang, "Non-orthogonal multiple access for 5G: Solutions, challenges, opportunities, and future research trends," *IEEE Commun. Mag.*, vol. 53, no. 9, pp. 74–81, Sep. 2015.

[2] Z. Ding *et al.*, "Application of non-orthogonal multiple access in LTE and 5G networks," *IEEE Commun. Mag.*, vol. 55, no. 2, pp. 185–191, Feb. 2017.

[3] S. M. R. Islam, N. Avazov, O. A. Dobre, and K.-S. Kwak, "Power-domain non-orthogonal multiple access (NOMA) in 5G systems: Potentials and challenges," *IEEE Commun. Surveys Tuts.*, vol. 19, no. 2, pp. 721–742, 2nd Quart., 2017.

[4] Y. Chen *et al.*, "Toward the standardization of non-orthogonal multiple access for next generation wireless networks," *IEEE Commun. Mag.*, vol. 56, no. 3, pp. 19–27, Mar. 2018.

[5] S. Verdú, *Multiuser Detection*. Cambridge, U.K.: Cambridge Univ. Press, 1998.

[6] J.-M. Kelif, J.-M. Gorce, and A. Gati, "Performance and energy in green superposition coding wireless networks: An analytical model," in *Proc. GLOBECOM*, Singapore, Dec. 2017, pp. 1–6.

[7] A. Benjebbour, Y. Saito, Y. Kishiyama, A. Li, A. Harada, and T. Nakamura, "Concept and practical considerations of non-orthogonal multiple access (NOMA) for future radio access," in *Proc. ISPACS*, Nov. 2013, pp. 770–774.

[8] S. Chen, B. Ren, Q. Gao, S. Kang, S. Sun, and K. Niu, "Pattern division multiple access—A novel nonorthogonal multiple access for fifth-generation radio networks," *IEEE Trans. Veh. Technol.*, vol. 66, no. 4, pp. 3185–3196, Apr. 2017.

[9] Z. Yuan, G. Yu, W. Li, Y. Yuan, X. Wang, and J. Xu, "Multi-user shared access for Internet of Things," in *Proc. IEEE VTC Spring*, May 2016, pp. 1–5.

[10] T. Cover, "Broadcast channels," *IEEE Trans. Inf. Theory*, vol. IT-18, no. 1, pp. 2–14, Jan. 1972.

[11] N. I. Miridakis and D. D. Vergados, "A survey on the successive interference cancellation performance for single-antenna and multiple-antenna OFDM systems," *IEEE Commun. Surveys Tuts.*, vol. 15, no. 1, pp. 312–335, 1st Quart., 2013.

[12] S. Vanka, S. Srinivasa, Z. Gong, P. Vizi, K. Stamatiou, and M. Haenggi, "Superposition coding strategies: Design and experimental evaluation," *IEEE Trans. Wireless Commun.*, vol. 11, no. 7, pp. 2628–2639, Jul. 2012.

[13] M. S. Ali, H. Tabassum, and E. Hossain, "Dynamic user clustering and power allocation for uplink and downlink non-orthogonal multiple access (NOMA) systems," *IEEE Access*, vol. 4, pp. 6325–6343, 2016.

[14] Z. Ding, Z. Yang, P. Fan, and H. V. Poor, "On the performance of non-orthogonal multiple access in 5g systems with randomly deployed users," *IEEE Signal Process. Lett.*, vol. 21, no. 12, pp. 1501–1505, Dec. 2014.

[15] Z. Yang, Z. Ding, P. Fan, and G. K. Karagiannidis, "On the performance of non-orthogonal multiple access systems with partial channel information," *IEEE Trans. Commun.*, vol. 64, no. 2, pp. 654–667, Feb. 2016.

[16] H. Pan, L. Lu, and S. C. Liew, "Practical power-balanced non-orthogonal multiple access," *IEEE J. Sel. Areas Commun.*, vol. 35, no. 10, pp. 2312–2327, Oct. 2017.

[17] L. Lu, L. You, and S. C. Liew, "Network-coded multiple access," *IEEE Trans. Mobile Comput.*, vol. 13, no. 12, pp. 2853–2869, Dec. 2014.

[18] L. You, S. C. Liew, and L. Lu, "Network-coded multiple access II: Toward real-time operation with improved performance," *IEEE J. Sel. Areas Commun.*, vol. 33, no. 2, pp. 264–280, Feb. 2015.

[19] H. Pan, L. Lu, and S. C. Liew, "Network-coded multiple access with higher-order modulations," in *Proc. IEEE Global Commun. Conf. (GLOBECOM)*, Dec. 2015, pp. 1–7.

[20] H. Pan, S. C. Liew, J. Liang, Y. Shao, and L. Lu, "Network-coded multiple access on unmanned aerial vehicle," *IEEE J. Sel. Areas Commun.*, vol. 36, no. 9, pp. 2071–2086, Sep. 2018.

[21] Z. Ding, M. Peng, and H. V. Poor, "Cooperative non-orthogonal multiple access in 5G systems," *IEEE Commun. Lett.*, vol. 19, no. 8, pp. 1462–1465, Aug. 2015.

[22] S. C. Liew, L. Lu, and S. Zhang, *A Primer on Physical-Layer Network Coding* (Synthesis Lectures on Communication Networks). San Rafael, CA, USA: Morgan & Claypool, 2015.

[23] S. Zhang, S. C. Liew, and P. P. Lam, "Hot topic: Physical-layer network coding," in *Proc. MobiCom*, Los Angeles, CA, USA, Jun. 2006, pp. 358–365.

[24] P. Chen, S. C. Liew, and L. Shi, "Bandwidth-efficient coded modulation schemes for physical-layer network coding with high-order modulations," *IEEE Trans. Commun.*, vol. 65, no. 1, pp. 147–160, Jan. 2017.

[25] S. C. Liew, S. Zhang, and L. Lu, "Physical-layer network coding: Tutorial, survey, and beyond," *Phys. Commun.*, vol. 6, pp. 4–42, Mar. 2013.

[26] P. Chen, Y. Fang, L. Wang, and F. C. M. Lau, "Decoding generalized joint channel coding and physical network coding in the LLR domain," *IEEE Signal Process. Lett.*, vol. 20, no. 2, pp. 121–124, Feb. 2012.

[27] L. Lu and S. C. Liew, "Asynchronous physical-layer network coding," *IEEE Trans. Wireless Commun.*, vol. 11, no. 2, pp. 819–831, Feb. 2012.

[28] S. Zhang and S.-C. Liew, "Channel coding and decoding in a relay system operated with physical-layer network coding," *IEEE J. Sel. Areas Commun.*, vol. 27, no. 5, pp. 788–796, Jun. 2009.

[29] T. Yang and J. Yuan, "Performance of iterative decoding for superposition modulation-based cooperative transmission," *IEEE Trans. Wireless Commun.*, vol. 9, no. 1, pp. 51–59, Jan. 2010.

[30] L. Shi, T. Yang, K. Cai, P. Chen, and T. Guo, "On MIMO linear physical-layer network coding: Full-rate full-diversity design and optimization," *IEEE Trans. Wireless Commun.*, vol. 17, no. 5, pp. 3498–3511, Mar. 2018.

[31] G. Cocco and S. Pfletschinger, "Seek and decode: Random multiple access with multiuser detection and physical-layer network coding," in *Proc. IEEE ICC*, Jun. 2014, pp. 501–506.

[32] T. Yang, L. Yang, Y. J. Guo, and J. Yuan, "A non-orthogonal multiple-access scheme using reliable physical-Layer network coding and cascade-computation decoding," *IEEE Trans. Wireless Commun.*, vol. 16, no. 3, pp. 1633–1645, Mar. 2017.

[33] J. Yuan, W. Feng, and B. Vucetic, "Performance of parallel and serial concatenated codes on fading channels," *IEEE Trans. Commun.*, vol. 50, no. 10, pp. 1600–1608, Oct. 2002.

[34] L. Shi, S. C. Liew, and L. Lu, "On the subtleties of q-PAM linear physical-layer network coding," *IEEE Trans. Inf. Theory*, vol. 62, no. 5, pp. 2520–2544, May 2016.

[35] S. Lin and D. J. Costello, Jr., *Error Control Coding: Fundamentals and Applications*, 2nd ed. Upper Saddle River, NJ, USA: Prentice-Hall, 2004.

[36] D. Divsalar, S. Dolinar, C. Jones, and K. Andrews, "Capacity approaching protograph codes," *IEEE J. Sel. Areas Commun.*, vol. 27, no. 6, pp. 876–888, Aug. 2009.

[37] Y. Fang, G. Bi, Y. L. Guan, and F. C. M. Lau, "A survey on protograph LDPC codes and their applications," *IEEE Commun. Surveys Tuts.*, vol. 17, no. 4, pp. 1989–2016, 4th Quart., 2015.

PINGPING CHEN (M'15) received the Ph.D. degree in electronic engineering from Xiamen University, China, in 2013. In 2012, he was a Research Assistant in electronic and information engineering with The Hong Kong Polytechnic University, Hong Kong. From 2013 to 2015, he was a Post-Doctoral Fellow at the Institute of Network Coding, The Chinese University of Hong Kong, Hong Kong. He is currently a Professor with Fuzhou University, China. His primary research interests include channel coding, joint source and channel coding, network coding, and UWB communications.

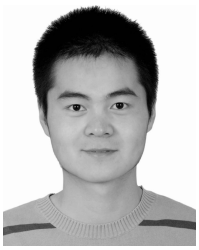

LONG SHI (S'10–M'13) received the Ph.D. degree in electrical engineering from the University of New South Wales, Sydney, Australia, in 2012. He was a Visiting Student at The Chinese University of Hong Kong and the University of Delaware in 2010 and 2011, respectively. From 2013 to 2016, he was a Post-Doctoral Fellow at the Institute of Network Coding, The Chinese University of Hong Kong. From 2014 to 2017, he was a Lecturer at the College of Electronic and Information Engineering, Nanjing University of Aeronautics and Astronautics. He is currently a Post-Doctoral Research Fellow at the Singapore University of Technology and Design. His current research interests include wireless network coding, wireless caching, and channel coding.

LITING GUO received the B.S. degree in radio technology and the M.S. degrees in communication and information system from Fuzhou University, China, in 1997, and 2000, respectively, and the Ph.D. degree in communication and information system from the University of Science and Technology of China in 2006. She is currently an Associate Professor with Fuzhou University. Her primary research interests include modulation, coding, channel estimation, and equalization in wireless communications.

ZHIFENG CHEN received the Ph.D. degree in electrical and computer engineering from the University of Florida, USA, in 2010. He is currently a Professor with the College of Physics and Information Engineering, Fuzhou University, China. His research interests include video coding, video transmission, computer vision, and machine learning.

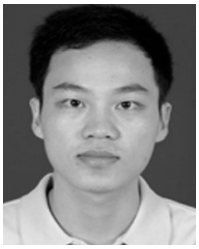

LINHUANG WU received the M.S. and Ph.D. degrees in communication and information system from Fuzhou University, Fuzhou, China, in 2009 and 2017, respectively. He is currently an Assistant Researcher with the College of Physics and Information Engineering, Fuzhou University. His research interests include digital predistortion of power amplifier linearization, computer vision, and machine learning.